# Synthesis, Helicity, and Chromism of Optically Active Poly(phenylacetylene)s Carrying Different Amino Acid Moieties and Pendant Terminal Groups

**Lo Ming Lai,[†] Jacky W. Y. Lam,[†] Anjun Qin,[†] Yongqiang Dong,[†,‡] and Ben Zhong Tang*[,†,‡]**

*Department of Chemistry, The Hong Kong University of Science & Technology, Clear Water Bay, Kowloon, Hong Kong, China, and Key Laboratory of Macromolecular Synthesis and Functionalization,[§] Department of Polymer Science & Engineering, Zhejiang University, Hangzhou, Zhejiang 310027, China*

*Received: December 9, 2005; In Final Form: April 10, 2006*

Functional phenylacetylene derivatives containing L-alanine and L-leucine moieties with chiral menthyl and achiral *n*-octyl terminal groups {HC≡C−$C_6H_4$-*p*-CONHCH(R)$CO_2$R′: R = $CH_3$, R′= (−)-(1*R*,2*S*,5*R*)-menthyl [**1**(−)]; R = $CH_2CH(CH_2)_3$, R′ = (−)-(1*R*,2*S*,5*R*)-menthyl [**2**(−)]; R′= $CH_2CH(CH_2)_3$, R′ = (+)-(1*S*,2*R*,5*S*)-menthyl [**2**(+)]; R′= $CH_2CH(CH_2)_3$, R′ = $(CH_2)_7CH_3$ (**2**o)} are synthesized. Polymerizations of the acetylene monomers are effected by organorhodium catalysts, giving corresponding polymers P**1**(−), P**2**(−), P**2**(+), and P**2**o of high molecular weights ($M_w$ up to $1.2 \times 10^6$) in high yields (up to 89%). The polymers are thermally stable ($T_d \geq 300$ °C) and soluble in common organic solvents. The polymer structures are characterized by IR, NMR, UV, and CD spectroscopies. Intense CD signals are observed in the visible spectral region, indicating that the polymer chains are taking a helical conformation with an excess of preferred handedness. The backbone conjugation and chain helicity of the polymers can be tuned by changing their molecular structures [(a)chiral pendant groups] and by applying external stimuli (solvent and pH). Addition of trifluoroacetic acid to the polymer solutions decreases their molar ellipticities and enhances their backbone conjugations, inducing a halochromism with a continuous and reversible color change (yellow ⇔ red).

## Introduction

Helicity is a structural feature of biological macromolecules and is expressed at all organizational levels of the molecular machineries of living systems.[1] Many biological functions performed by the natural polymers are associated with their hierarchical structures, whose formation is largely regulated by the helical conformation of the polymer chains as well as the folding and assembling information encoded in their building blocks.[1,2] Development of synthetic biomimetic helical polymers is a topic of great current interest.[3−5] Studies of the simple unnatural systems may lead to a better understanding of the complex natural systems. Helical polymers with extended electronic conjugations are under hot pursuits of scientists due to their potential technological applications as optical polarizing films, chiral stationary phases, asymmetric electrodes, anisotropic molecular wires, fluorescent chemosensors, and so forth.[6−9]

From the viewpoint of molecular design, the best building blocks for the construction of biomimetic macromolecules are the naturally occurring species with molecular asymmetry and hydrogen-bonding capacity. We have prepared a large variety of conjugated helical polymers comprised of polyacetylene backbones and amino acid, sterol, saccharide, and nucleoside appendages.[3a,10−12] We have found that the amphiphilic polyacetylenes exhibit very large chain helicity, which can be continuously and reversibly modulated by such simple external stimuli as solvent, pH, temperature, and achiral additives.

**CHART 1**

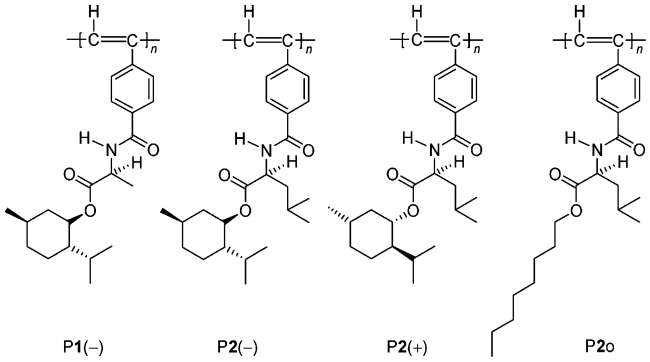


Although the polymers are homopolymers (rather than block copolymers), they can self-assemble into biomimetic supramolecular structures including spherical pearls, twisted cables, and helical nanotubes on all length scales and spatial dimensionalities.[3a,5f]

In our previous investigations, the polymers contain only a single type of stereogenic block in their monomer repeat units. As an extension of our research program in the area, we have recently embarked on the design and synthesis of helical polyacetylenes with multiple stereogenic centers in their repeating units.[11] To generate more helical polyacetylenes with new structures and to gain information on their structure−property relationships, in this work, we integrated different stereogenic pendants and (a)chiral terminal groups into the molecular structure of poly(phenylacetylene) (Chart 1). We studied the helical structures of the resultant polymers in an effort to learn how the pendant groups with different chirality and bulkiness as well as the environmental variations will affect their chiroptical properties.

* Corresponding author. Phone: +852-2358-7375. Fax: +852-2358-1594. E-mail: tangbenz@ust.hk.
† The Hong Kong University of Science & Technology.
‡ Zhejiang University.
§ Administrated by the Ministry of Education of the People's Republic of China.

10.1021/jp057179q CCC: $33.50 
Published on Web 05/25/2006

**SCHEME 1**

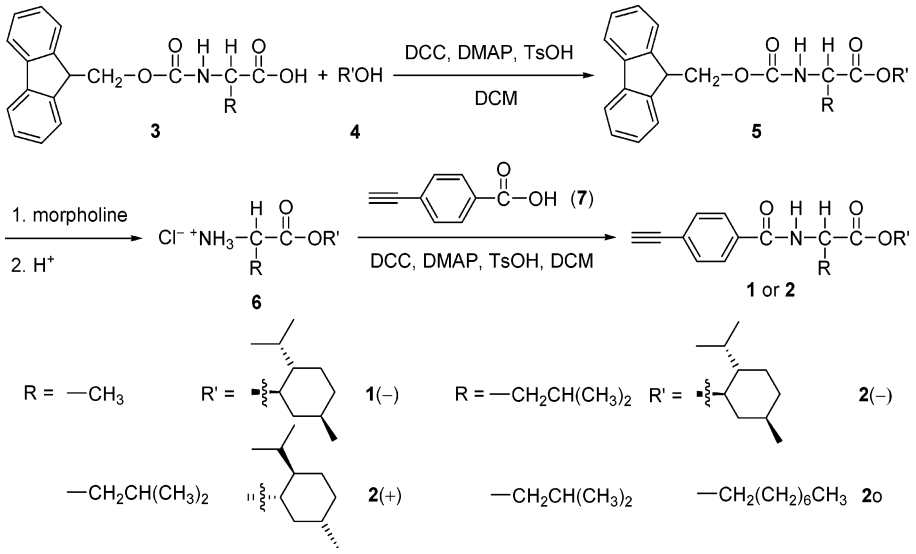


## Experimental Section

**Materials.** Toluene (BDH) and THF (Lab-Scan) were distilled from sodium benzophenone ketyl immediately prior to use. Chloroform and dichloromethane (DCM) were purchased from Lab-Scan and distilled over calcium hydride. Triethylamine was distilled and dried over potassium hydroxide. *N*,*N*′-Dicyclohexylcarbodiimide (DCC), 4-(dimethylamino)pyridine (DMAP), (1*S*,2*R*,5*S*)-(+)-menthol (all from International Laboratory), *p*-toluenesulfonic acid monohydrate (TsOH), (1*R*,2*S*,5*R*)-(−)-menthol, diethylamine (all from Aldrich), 1-octanol (Nacalai Tesque), *N*-(9-fluorenylmethoxycarbonyl)-L-alanine, and *N*-(9-fluorenylmethoxycarbonyl)-L-leucine (both from GL Biochem) were used as received. Organorhodium complexes $[Rh(nbd)Cl]_2$, $[Rh(cod)Cl]_2$, and $Rh(cod)(NH_3)Cl$ (where nbd = 2,5-norborndiene and cod = 1,5-cyclooctadiene) were prepared by literature methods.[13] 4-Ethynylbenzonic acid (**7**) was synthesized according to published procedures.[14]

**Instrumentation.** IR spectra were measured on a Perkin-Elmer Spectrum One spectrophotometer. $^1H$ and $^{13}C$ NMR spectra were recorded on a Bruker ARX 300 NMR spectrometer with chloroform-*d* as solvent and tetramethylsilane ($\delta = 0$) as internal reference. Mass spectra were recorded on a Finnign TSQ 7000 triple-quadrupole mass spectrometer operating in a chemical ionization (CI) mode with methane as carrier gas. Elemental analyses were performed on a VARIO EL3 CHNOS elemental analyzer. Molecular weights and polydispersity indexes ($M_w/M_n$) of the polymers were estimated in THF by a Waters Associated gel permeation chromatography (GPC) system. A set of monodisperse polystyrene standards covering the molecular weight range of $10^3-10^7$ was used for the molecular weight calibration. Thermal stability of the polymers was evaluated on a Perkin-Elmer thermogravimetric analyzer TGA 7 under nitrogen at a heating rate of 20 deg/min. Specific optical rotation ($[\alpha]^{23}_D$) was recorded on a Perkin-Elmer 241 polarimeter at 23 °C (room temperature), using the D-line of the sodium lamp (589.3 nm) as the monochromatic light source. UV spectra were measured on a Milton Roy Spectronic 3000 Array spectrophotometer and molar absorptivity ($\epsilon$) of the polymer was calculated on the basis of its repeat unit. Circular dichroism (CD) spectra were taken on a Jasco-720 spectropolarimeter in 1 mm quartz cuvettes (step resolution: 0.2 nm; scan speed: 50 nm/min; sensitivity: 0.1°; response time: 0.5 s). Each spectrum was the average of 5−10 scans. The molar ellipticity ($[\theta]$) of the polymer was calculated on the basis of its monomer repeat unit.

**Monomer Synthesis.** The phenylacetylene derivatives containing amino acid moieties with different (a)chiral terminal groups were prepared by multistep synthetic routes (Scheme 1). The experimental procedures for the synthesis of **1**(−) are given below as examples [for simplicity, the numbers denoting the intermediates (**3**−**5**) are used directly with R and R′ representing methyl and (1*R*,2*S*,5*R*)-(−)-menthyl groups, respectively, in the following descriptions].

*N*-(*9-Fluorenylmethoxycarbonyl*)-L-*alanine* (*1R,2S,5R*)-(−)-*Menthyl Ester* (*5*). Into a 500 mL round-bottom flask were added 1.9 g of (1*R*,2*S*,5*R*)-(−)-menthol (12.2 mmol), 2.2 g of DCC (10.7 mmol), 0.58 g of DMAP (4.8 mmol), and 0.37 g of TsOH (1.9 mmol) in 300 mL of dry DCM under stirring. After a clear mixture was formed, 3.0 g (9.6 mmol) of *N*-(9-fluorenylmethoxycarbonyl)-L-alanine (**3**) was added. The resulting solution was stirred at room temperature for 24 h and the solvent was removed by a rotary evaporator. The crude product was purified on a silica gel column with a chloroform/hexane mixture (10:1 by volume) as eluent. Product **5** was isolated as a white solid in 84.2% yield (3.65 g).

*4-Ethynylbenzoyl*-L-*alanine* (*1R,2S,5R*)-(−)-*Menthyl Ester* [***1***(−)]. In a 250 mL round-bottom flask was dissolved 3.5 g of **5** in 100 mL of dry DCM. Morpholine (20 mL) was added and the resultant mixture was stirred for 35 min. Dilute hydrochloric acid (20 mL) was added to quench the reaction. The mixture was diluted with 200 mL of chloroform and then washed with 200 mL of water two times. After solvent evaporation, the crude product was purified on a silica gel column with pure chloroform then methanol as eluents. A yellow liquid of **6** was obtained in 47.7% yield (0.98 g).

Into another 500 mL round-bottom flask were added 0.98 g (3.7 mmol) of **6**, 1.3 g (6.3 mmol) of DCC, 0.3 g (2.5 mmol) of DMAP, and 0.2 g (1.1 mmol) of TsOH in 250 mL of dry DCM. After gentle stirring, 0.8 g (5.5 mmol) of 4-ethynylbenzoic acid (**7**) was added. After 24 h, the formed urea salts were filtrated and the filtrate was condensed. The crude monomer was purified on a silica gel column with a mixture of chloroform and acetone (15:1 by volume) as eluent. A white solid of **1**(−) was isolated in 72.3% yield. IR (KBr) $\nu$ ($cm^{-1}$) 3303 (N−H and ≡C−H stretchings), 2108 (C≡C stretching), 1730 (C═O

ester stretching), 1645 (C═O amide stretching), 1609 (N−H bending). $^1$H NMR (300 MHz, $CDCl_3$) $\delta$ (TMS, ppm) 7.8 [d, 2H, aromatic protons ortho (*o*) to C═O], 7.6 [d, 2H, aromatic protons meta (*m*) to C═O], 6.9 (d, 1H, NH), 4.8 (m, 2H, NHC*H* and OCH), 3.2 (s, 1H, HC≡), 2.0 (m, 1H), 1.9 (m, 1H), 1.8 (m, 2H), 1.5 (m, 4H), 1.2−0.8 (m, 13H). $^{13}$C NMR (75 MHz, $CDCl_3$) $\delta$ (TMS, ppm) 172.9 ($CO_2$), 166.0 (CONH), 134.1 (aromatic carbon attached to C═O), 132.4 (aromatic carbons *m* to C═O), 127.1 (aromatic carbons *o* to C═O), 125.6 [aromatic carbons para (*p*) to C═O], 82.9 (Ph*C*≡), 79.7 (HC≡), 75.9 (OCH), 60.7 (CO*C*HNH), 48.7, 47.0, 40.7, 34.2, 31.5, 26.4, 23.5, 22.1, 20.8, 18.9, 16.4. MS (CI) *m*/*z* 356.2 [(M + 1)$^+$, calcd 356.2]. Anal. Calcd for $C_{22}H_{29}NO_3$: C, 74.33; H, 8.22; N, 3.94; O, 13.50. Found: C, 74.12; H, 8.32; N, 3.92.

Other monomers (**2**) were synthesized with experimental procedures similar to those described above for the preparation of monomer **1**(−). Their characterization data are given below.

*4-Ethynylbenzoyl*-L-*leucine* (*1R,2S,5R*)-(−)-*Menthyl Ester* [*2*(−)]. White solid; 69.3% yield. IR (KBr) $\nu$ (cm$^{-1}$) 3305 (N−H and ≡C−H stretchings), 2108 (C≡C stretching), 1722 (C═O ester stretching), 1646 (C═O amide stretching), 1609 (N−H bending). $^1$H NMR (300 MHz, $CDCl_3$) $\delta$ (TMS, ppm) 7.7 (d, 2H, aromatic protons *o* to C═O), 7.5 (d, 2H, aromatic protons *m* to C═O), 6.9 (d, 1H, NH), 4.8 (m, 2H, NHC*H*CO and OCH), 3.2 (s, 1H, HC≡), 1.9 (m, 2H), 1.7 (m, 5H), 1.5 (m, 1H), 1.0 (m, 16H), 0.8 (m, 3H). $^{13}$C NMR (75 MHz, $CDCl_3$) $\delta$ (TMS, ppm) 173.7 ($CO_2$), 166.8 (CONH), 134.5 (aromatic carbon attached to C═O), 132.8 (aromatic carbons *m* to C═O), 127.6 (aromatic carbons *o* to C═O), 126.1 (aromatic carbons *p* to C═O), 83.4 (Ph*C*≡), 80.1 (HC≡), 76.3 (OCH), 51.9 (CO*C*HNH), 47.5, 42.5, 41.3, 34.8, 32.0, 26.8, 25.7, 24.0, 23.6, 22.8, 22.6, 21.3, 16.9. MS (CI) *m*/*z* 398.3 [(M + 1)$^+$, calcd 398.3]. Anal. Calcd for $C_{25}H_{35}NO_3$: C, 75.53; H, 8.87; N, 3.52; O, 12.07. Found: C, 74.13; H, 8.79; N, 3.55.

*4-Ethynylbenzoyl*-L-*leucine* (*1S,2R,5S*)-(+)-*Menthyl Ester* [*2*(+)]. White solid; 76.3% yield. IR (KBr) $\nu$ (cm$^{-1}$) 3306 (N−H and ≡C−H stretchings), 2109 (C≡C stretching), 1731 (C═O ester stretching), 1645 (C═O amide stretching), 1609 (N−H bending). $^1$H NMR (300 MHz, $CDCl_3$) $\delta$ (TMS, ppm) 7.7 (d, 2H, aromatic protons *o* to C═O), 7.6 (d, 2H, aromatic protons *m* to C═O), 6.6 (d, 1H, NH), 4.8 (m, 2H, NHC*H*CO and OCH), 3.2 (s, 1H, HC≡), 2 (m, 1H), 1.9 (m, 1H), 1.7 (m, 5H), 1.5 (m, 1H), 1.1 (m, 10H), 0.9 (m, 6H), 0.8 (m, 3H). $^{13}$C NMR (75 MHz, $CDCl_3$) $\delta$ (TMS, ppm) 172.7 ($CO_2$), 166.0 (CONH), 134.0 (aromatic carbon attached to C═O), 132.3 (aromatic carbons *m* to C═O), 127.0 (aromatic carbons *o* to C═O), 125.5 (aromatic carbons *p* to C═O), 82.7 (Ph*C*≡), 79.3 (HC≡), 75.9 (OCH), 51.7 (CO*C*HNH), 46.9, 41.9, 40.7, 34.1, 31.4, 26.0, 25.1, 23.0, 22.1, 22.0, 20.8, 15.8. MS (CI) *m*/*z* 398.3 [(M + 1)$^+$, calcd 398.3]. Anal. Calcd for $C_{25}H_{35}NO_3$: C, 75.53; H, 8.87; N, 3.52; O, 12.07. Found: C, 75.49; H, 9.02; N, 3.56.

*4-Ethynylbenzoyl*-L-*leucine Octyl Ester* (*2o*). White solid; 70.1% yield. IR (KBr) $\nu$ (cm$^{-1}$) 3358 (N−H and ≡C−H stretchings), 2109 (C≡C stretching), 1739 (C═O ester stretching), 1645 (C═O amide stretching), 1609 (N−H bending). $^1$H NMR (300 MHz, $CDCl_3$) $\delta$ (TMS, ppm) 7.8 (d, 2H, aromatic protons *o* to C═O), 7.6 (d, 2H, aromatic protons *m* to C═O), 6.6 (d, 1H, NH), 4.8 (m, 1H, NHC*H*CO), 4.2 (m, 2H, $CO_2$-$CH_2$), 3.2 (s, 1H, HC≡), 1.7 (m, 5H), 1.2 (m, 6H), 1.0 (m, 10H), 0.9 (m, 3H). $^{13}$C NMR (75 MHz, $CDCl_3$) $\delta$ (TMS, ppm) 174.0 ($CO_2$), 166.9 (CONH), 134.6 (aromatic carbon attached to C═O), 133.0 (aromatic carbons *m* to C═O), 127.7 (aromatic carbons *o* to C═O), 126.2 (aromatic carbons *p* to C═O), 83.4 (Ph*C*≡), 80.3 (HC≡), 66.4 ($CO_2CH_2$), 52.0 (CO*C*HNH), 46.6, 32.4, 29.8, 29.2, 26.5, 25.7, 23.5, 23.3, 22.8, 14.8. MS (CI) *m*/*z* 372.3 [(M + 1)$^+$, calcd 372.3]. Anal. Calcd for $C_{23}H_{33}NO_3$: C, 74.36; H, 8.95; N, 3.77; O, 12.92. Found: C, 74.32; H, 9.08; N, 4.01.

**TABLE 1: Polymerization of 4-Ethynylbenzoyl-L-alanine (1*R*,2*S*,5*R*)-(−)-Menthyl Ester [1(−)]**[a]

| no. | catalyst[b] | solvent[b] | yield (%) | $M_w$[c] | $M_w/M_n$[c] |
|---|---|---|---|---|---|
| 1 | $[Rh(nbd)Cl]_2$ | THF/$Et_3N$ | 82.9 | 1 211 000 | 9.5 |
| 2 | $[Rh(nbd)Cl]_2$ | DCM/$Et_3N$ | 88.6 | 1 208 000 | 8.2 |
| 3 | $[Rh(cod)Cl]_2$ | THF/$Et_3N$ | 69.3 | 810 000 | 8.8 |
| 4 | $[Rh(cod)Cl]_2$ | DCM/$Et_3N$ | 74.1 | 346 000 | 4.6 |
| 5 | $Rh(cod)(NH_3)Cl$ | THF | 82.0 | 426 000 | 4.6 |
| 6 | $Rh(cod)(NH_3)Cl$ | DCM | 86.2 | 295 000 | 4.1 |

[a] Carried out at room temperature in air for 24 h; $[M]_0$ = 0.2 M, [cat.] = 0.2 mM. [b] Abbreviations: nbd = 2,5-norborndiene, cod = 1,5-cyclooctadiene, DCM = dichloromethane. Solvent/$Et_3N$ = 10:1 (v/v). [c] Determined by GPC in THF on the basis of a polystyrene calibration.

**TABLE 2: Polymerization of 4-Ethynylbenzoyl-L-leucine (1*R*,2*S*,5*R*)-(−)-Menthyl Ester [2(−)]**[a]

| no. | catalyst[b] | solvent[b] | yield (%) | $M_w$[c] | $M_w/M_n$[c] |
|---|---|---|---|---|---|
| 1 | $[Rh(nbd)Cl]_2$ | THF/$Et_3N$ | 62.7 | 237 100 | 3.1 |
| 2 | $[Rh(nbd)Cl]_2$ | DCM/$Et_3N$ | 49.3 | 294 500 | 2.4 |
| 3 | $[Rh(cod)Cl]_2$ | THF/$Et_3N$ | 48.9 | 157 900 | 2.6 |
| 4 | $[Rh(cod)Cl]_2$ | DCM/$Et_3N$ | 71.0 | 128 300 | 3.0 |
| 5 | $Rh(cod)(NH_3)Cl$ | THF | 36.7 | 155 800 | 3.1 |
| 6 | $Rh(cod)(NH_3)_3Cl$ | DCM | 41.5 | 135 100 | 3.3 |

[a] Carried out at room temperature in air for 24 h; $[M]_0$ = 0.2 M, [cat.] = 0.2 mM. [b] Abbreviations: nbd = 2,5-norborndiene, cod = 1,5-cyclooctadiene, DCM = dichloromethane. Solvent/$Et_3N$ = 10:1 (v/v). [c] Determined by GPC in THF on the basis of a polystyrene calibration.

**Polymerization.** All the polymerization reactions and manipulations were carried out in air at room temperature. Typical experimental procedures for the polymerization of **1**(−) by $[Rh(nbd)Cl]_2$ are given below as examples.

*Poly*[*4-ethynylbenzoyl*-L-*alanine* (*1R,2S,5R*)-(−)-*menthyl ester*][*P1*(−)]. Into a 25 mL test tube was added 0.43 g (1.2 mmol) of **1**(−) in 6 mL of a triethylamine/THF mixture (1:10 v/v) in air under stirring. After the monomer was completely dissolved, 0.014 g (0.03 mmol) of $[Rh(nbd)Cl]_2$ was added. The resultant mixture was stirred overnight at room temperature. The mixture was diluted by 5 mL of THF and added dropwise to 450 mL of an acetone/methanol mixture (1:5 by volume) through a cotton filter. The precipitate was filtered through a Gooch crucible and washed with the acetone/methanol mixture several times. The polymer was dried under reduced pressure and obtained in 82.9% yield as an orange-yellow fibrous solid. $M_w$ 1 211 000; $M_w/M_n$ 9.5 (GPC, polystyrene calibration; Table 1, no.1). IR (KBr) $\nu$ (cm$^{-1}$) 3435 (N−H stretching), 1740 (C═O ester stretching), 1648 (C═O amide stretching), 1609 (N−H bending). $^1$H NMR (300 MHz, $CDCl_3$) $\delta$ (TMS, ppm) 7.7 (NH), 7.3 (aromatic protons *o* to C═O), 6.1 (aromatic protons *m* to C═O), 5.8 (*Z* olefin proton), 4.7 (NHC*H*), 2.4, 1.3, 0.9. $^{13}$C NMR (75 MHz, $CDCl_3$) $\delta$ (TMS, ppm) 172.5 ($CO_2$), 126.3 (aromatic protons), 57.7 (CONH), 47.0, 40.6, 31.4, 22.0, 20.7, 17.5, 16.2.

*Poly*[*4-ethynylbenzoyl*-L-*leucine* (*1R,2S,5R*)-(−)-*menthyl ester*][*P2*(−)]. Orange fibrous solid; yield 62.7%. $M_w$ 237 100; $M_w/M_n$ 3.1 (GPC, polystyrene calibration; Table 2, no. 1). IR (KBr) $\nu$ (cm$^{-1}$) 3434 (N−H stretching), 1735 (C═O ester stretching), 1648 (C═O amide stretching), 1608 (N−H bending). $^1$H NMR (300 MHz, $CDCl_3$) $\delta$ (TMS, ppm) 7.6 (NH), 6.9 (aromatic protons *o* to C═O), 6.4 (aromatic protons *m* to C═O), 5.5 (*Z* olefin proton), 4.6 (NHC*H*), 3.0, 1.7, 1.6, 0.9. $^{13}$C NMR (75 MHz, $CDCl_3$) $\delta$ (TMS, ppm) 172.6 ($CO_2$), 166.1

**TABLE 3: Polymerization of 4-Ethynylbenzoyl-L-leucine (1*S*,2*R*,5*S*)-(+)-Menthyl Ester [2(+)][a]**

| no. | catalyst[b] | solvent[b] | yield (%) | $M_w$[c,d] | $M_w/M_n$[c,d] |
|---|---|---|---|---|---|
| 1 | $[Rh(nbd)Cl]_2$ | $THF/Et_3N$ | 72.9 | 82 000 | 2.3 |
| 2 | $[Rh(nbd)Cl]_2$ | $DCM/Et_3N$ | 67.8 | 81 000 | 2.3 |
| 3 | $[Rh(cod)Cl]_2$ | $THF/Et_3N$ | 70.6 | 61 000 | 2.2 |
| 4 | $[Rh(cod)Cl]_2$ | $DCM/Et_3N$ | 75.6 | 75 000 | 2.3 |
| 5 | $Rh(cod)(NH_3)Cl$ | THF | 66.1 | 68 000 | 2.3 |
| 6 | $Rh(cod)(NH_3)Cl$ | DCM | 83.5 | 127 000 | 2.7 |

[a] Carried out at room temperature in air for 24 h; $[M]_0 = 0.2$ M, [cat.] = 0.2 mM. [b] Abbreviations: nbd = 2,5-norborndiene, cod = 1,5-cyclooctadiene, DCM = dichloromethane. Solvent/$Et_3N$ = 10:1 (v/v). [c] Determined by GPC in THF on the basis of a polystyrene calibration. [d] For the THF-soluble fraction.

**TABLE 4: Polymerization of 4-Ethynylbenzoyl-L-leucine Octyl Ester (2o)[a]**

| no. | catalyst[b] | solvent[b] | yield (%) | $M_w$[c] | $M_w/M_n$[c] |
|---|---|---|---|---|---|
| 1 | $[Rh(nbd)Cl]_2$ | $THF/Et_3N$ | 85.7 | 234 800 | 4.6 |
| 2 | $[Rh(nbd)Cl]_2$ | $DCM/Et_3N$ | 83.7 | 299 900 | 5.1 |
| 3 | $[Rh(cod)Cl]_2$ | $THF/Et_3N$ | 73.8 | 113 000 | 4.3 |
| 4 | $[Rh(cod)Cl]_2$ | $DCM/Et_3N$ | 83.2 | 151 600 | 3.2 |
| 5 | $Rh(cod)(NH_3)Cl$ | THF | 81.5 | 139 000 | 3.9 |
| 6 | $Rh(cod)(NH_3)Cl$ | DCM | 82.8 | 92 200 | 2.9 |

[a] Carried out at room temperature in air for 24 h; $[M]_0 = 0.2$ M, [cat.] = 0.2 mM. [b] Abbreviations: nbd = 2,5-norborndiene, cod = 1,5-cyclooctadiene, DCM = dichloromethane. Solvent/$Et_3N$ = 10:1 (v/v). [c] Determined by GPC in THF on the basis of a polystyrene calibration.

(CONH), 127.3 (aromatic protons), 74.5, 51.4, 46.9, 40.6, 34.1, 31.4, 25.0, 22.5, 22.0, 20.8, 16.3.

*Poly*[*4-ethynylbenzoyl*-L-*leucine* (*1S,2R,5S*)-(+)-*menthyl ester*] [*P2*(+)]. Reddish yellow fibrous solid; yield 72.9%. $M_w$ 82 000; $M_w/M_n$ 2.3 (GPC, THF soluble fraction, polystyrene calibration; Table 3, no. 1). IR (KBr) $\nu$ ($cm^{-1}$) 3434 (N−H stretching), 1732 (C═O ester stretching), 1648 (C═O amide stretching), 1609 (N−H bending). $^1H$ NMR (300 MHz, $CDCl_3$) $\delta$ (TMS, ppm) 7.6 (NH), 7 (aromatic protons *o* to C═O), 6.3 (aromatic protons *m* to C═O), 5.5 (*Z* olefin proton), 4.6 (NHC*H*), 2.8, 1.7, 1.4, 0.9. $^{13}C$ NMR (75 MHz, $CDCl_3$) $\delta$ (TMS, ppm) 172.4 ($CO_2$), 127.5 (aromatic protons), 51.9, 46.8, 41.9, 31.4, 25.9, 22.4, 20.8, 15.8.

*Poly*(*4-ethynylbenzoyl*-L-*leucine octyl ester*) (*P2o*). Orange-yellow powder; yield 85.7%. $M_w$ 234 800; $M_w/M_n$ 4.6 (GPC, polystyrene calibration; Table 4, no. 1). IR (KBr) $\nu$ ($cm^{-1}$) 3294 (N−H stretching), 1743 (C═O ester stretching), 1640 (C═O amide stretching), 1608 (N−H bending). $^1H$ NMR (300 MHz, $CDCl_3$) $\delta$ (TMS, ppm) 7.6 (NH), 6.6 (aromatic protons *o* to C═O), 6.2 (aromatic protons *m* to C═O), 5.6 (*Z* olefin proton), 4.6 (NHC*H*), 4.1 ($CO_2CH_2$), 2.8, 1.6, 1.3, 0.9. $^{13}C$ NMR (75 MHz, $CDCl_3$) $\delta$ (TMS, ppm) 173.0 ($CO_2$), 166 (CONH), 127.6 (aromatic protons), 65.1, 51.3, 41.0, 31.8, 29.2, 28.5, 25.9, 24.9, 22.6, 22.0, 14.0.

## Results and Discussion

**Monomer Preparation.** We designed molecular structures of four phenylacetylene derivatives containing different amino acid moieties and (a)chiral terminal groups and elaborated multistep reaction routes for their syntheses (Scheme 1). We first esterified the *N*-(9-fluorenylmethoxycarbonyl) (Fmoc)-protected amino acids (**3**) with alcohols **4** in the presence of DCC, DMAP, and TsOH. Fmoc is a common amino acid protecting group in peptide and glycopeptide syntheses because it is stable to the glycosylation conditions. It can be easily removed under mild conditions by such bases as morpholine and piperidine,[15] giving products with free amino functionality. The Fmoc groups in **5** were cleaved by a morpholine/DCM mixture, generating **6** upon acidification. Amidation of 4-ethynylbenzoic acid (**7**) with **6** produced the desirable monomers **1** and **2** in 69−76% yields after purification by column chromatography. The monomers were characterized by spectroscopic methods and satisfactory analysis data corresponding to their molecular structures were obtained (see the Experimental Section for details).

**Polymer Synthesis.** Since organorhodium complexes are effective catalysts for the polymerizations of phenylacetylenes,[11,16] we studied the polymerizations of our monomers using the rhodium−diene type complexes.

As can be seen from Table 1, the polymerizations of **1**(−) catalyzed by $[Rh(nbd)Cl]_2$ in $THF/Et_3N$ and $DCM/Et_3N$ both afford polymers with very high molecular weights ($>1.2 \times 10^6$) in high yields (≥83%). Encouraged by the results of $[Rh(nbd)Cl]_2$, we checked the catalytic activities of other Rh complexes with different ligands. $[Rh(cod)Cl]_2$ also works well for the acetylene polymerization in $THF/Et_3N$ and $DCM/Et_3N$, furnishing polymers with $M_w$ up to $8.1 \times 10^5$ in over 70% yields. Satisfactory results are obtained by $Rh(cod)(NH_3)Cl$ in pure THF and DCM, thanks to the internally coordinated amine ligand, which helps improve the performance of the polymerization catalyst. The molecular weight is sensitive to the polymerization solvent, with the $M_w$ of the polymer obtained in THF being ~1.4-fold higher than that in DCM.

The polymerization behaviors of **2**(−) are similar to those of **1**(−). All the organorhodium complexes, namely, $[Rh(nbd)Cl]_2$, $[Rh(cod)Cl]_2$, and $Rh(cod)(NH_3)Cl$, effectively initiate the polymerization of **2**(−) (Table 2). Compared to its counterparts with cod ligand, the rhodium complex with nbd ligand gives generally better polymerization results. The polymerization catalyzed by $[Rh(nbd)Cl]_2$ in $DCM/Et_3N$ produces a polymer with the highest $M_w$ ($\sim 3.0 \times 10^5$) in a satisfactory yield (49.3%) (Table 2, no. 2). Again the Rh complex with internally coordinated amine ligand works well as the catalyst in the pure solvents in the absence of externally added amine species (Table 2, nos. 5 and 6).

Monomer **2**(+) is a diastereoisomer of monomer **2**(−) with a terminal group of opposite chirality. Its Rh-catalyzed polymerizations all proceed well, producing polymers in high yields (66−84%; Table 3). However, compared to P**2**(−), P**2**(+) has a much poorer solubility in common organic solvents (vide post). Similar to **2**(−), **2**o can be effectively polymerized by the organorhodium catalysts (Table 4). $[Rh(nbd)Cl]_2$ in $DCM/Et_3N$ is the best catalytic system for the polymerization, giving a polymer with an $M_w$ of $3 \times 10^5$ in a high yield (83.7%).

**Structural Characterization.** The structures of the polymers are characterized spectroscopically. An example of the IR spectrum of polymer P**2**o is shown in Figure 1 along with that of its monomer **2**o. The monomer exhibits absorption bands at 3258 and 2109 $cm^{-1}$ associated with the ≡C−H and C≡C stretching vibrations, respectively (Figure 1A). These peaks are not observed in the spectrum of P**2**o, suggesting that the acetylene triple bond of **2**o has been consumed by the polymerization reaction.

Figure 2 shows the $^1H$ NMR spectrum of a chloroform solution of P**2**o along with that of its monomer **2**o. The spectrum of P**2**o shows no resonance peak of acetylene proton at $\delta$ 3.2 but is poorly resolved, making it difficult to elucidate its molecular structure. The broad peaks are probably due to the existence of multiple intra- and interchain hydrogen bonds in the polymer in the solvent. The hydrogen bonds may induce the macromolecular chains to aggregate. The motions of the

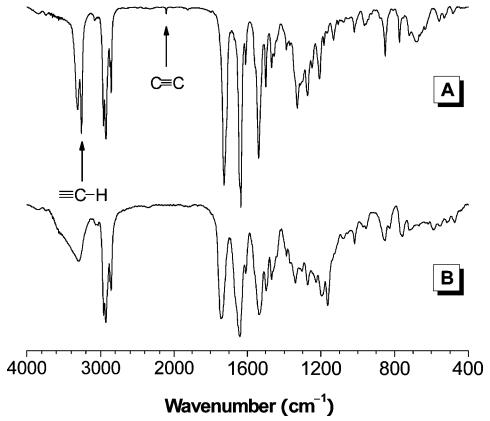


**Figure 1.** IR spectra of (A) monomer **2**o and (B) its polymer P**2**o (sample from Table 4, no. 1).

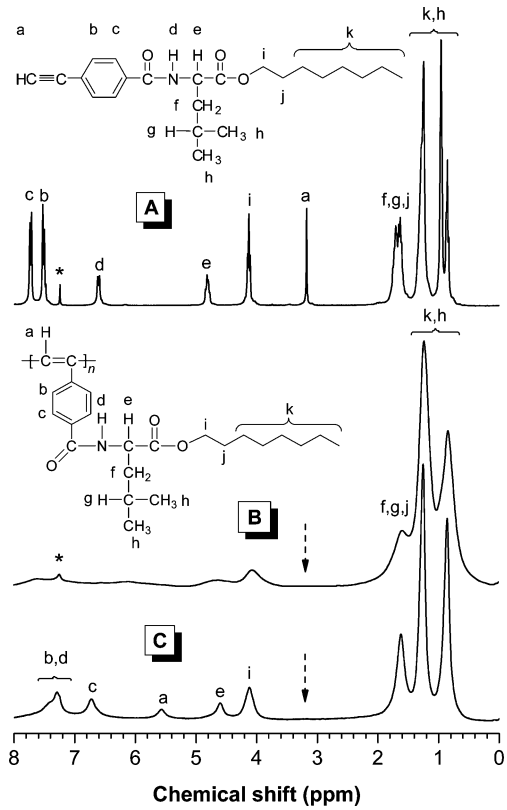


**Figure 2.** $^{1}$H NMR spectra of (A) **2**o and (B and C) its polymer P**2**o (sample from Table 4, no. 1) in chloroform-*d* containing (A and B) 0 and (C) 10 vol % of trifluoroacetic acid. The solvent peaks are marked with asterisks.

protons in the polymer aggregates are restricted, thus increasing the relaxation times and broadening the resonance peaks.

When 10 vol % of trifluoroacetic acid (TFA) is added, a better-resolved spectrum is obtained, where the resonances of the amide and olefinic protons of the polymer with a *Z-s-E* conformation are observed at $\delta \sim 7.3$ and $\sim 5.8$, respectively.[11,17] The carboxylic group of the TFA molecule may form hydrogen bonds with the amide and ester groups of the polymer solute. This helps to solvate the macromolecular chains and to partially disassemble the clusters of polymer aggregates, thus making the spectrum of the polymer better resolved.

The $^{13}$C NMR spectra of P**2**o and **2**o in deuterated chloroform are shown in Figure 3. While the acetylene carbons of **2**o resonate at $\delta$ 83.4 and 80.3, these peaks are completely absent in the spectrum of its polymer P**2**o. Again due to its chain

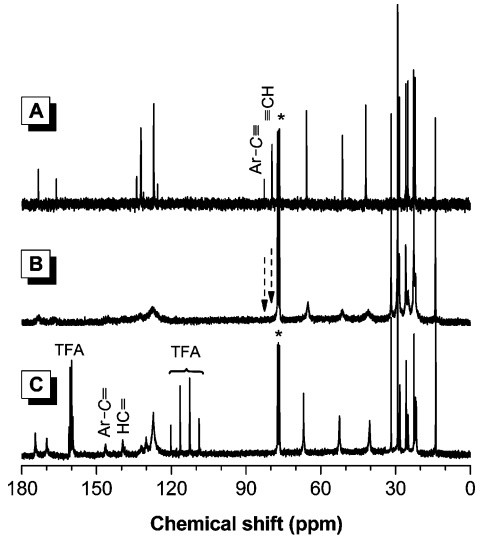


**Figure 3.** $^{13}$C NMR spectra of (A) **2**o and (B and C) its polymer P**2**o (sample from Table 4, no. 1) in chloroform-*d* containing (A and B) 0 and (C) 10 vol % of trifluoroacetic acid (TFA). The solvent peaks are marked with asterisks.

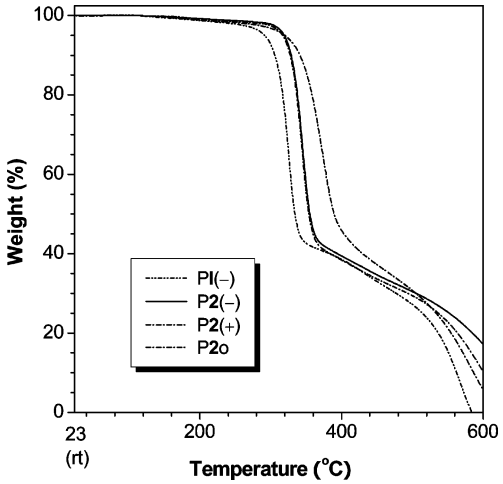


**Figure 4.** TGA thermograms of P**1**(−) (sample from Table 1, no. 1), P**2**(−) (Table 2, no. 1), P**2**(+) (Table 3, no. 1), and P**2**o (Table 4, no. 1) recorded under nitrogen at a heating rate of 20 deg/min.

aggregation, the spectrum of the polymer measured in pure chloroform-*d* is poorly resolved, giving broad resonance peaks with low intensities. When the solvation of macromolecular chains is enhanced by the addition of TFA, their resonance peaks are sharpened and intensified (Figure 3C). The resonance peaks of the olefinic carbons of the polyene backbone of the polymer become discernible at $\delta$ 146.6 and 139.5. No other unexpected signals are found and all the resonance peaks can be readily assigned, confirming that the molecular structure of the polymer is indeed P**2**o, as shown in Chart 1.

**Stability and Solubility.** Notwithstanding the high conductivity of its doped form,[18] polyacetylene has found few practical applications because of its notorious instability and intractability. All of our polymers are, however, thermally stable and solution-processable. As shown in Figure 4, almost no weight losses are recorded when the polymers are heated to 300 °C. The temperatures for initial weight losses ($T_d$) for the polymers containing L-leucine moiety (P**2**) are all higher than that for the polymer containing L-alanine moiety (P**1**). All the P**2** polymers, i.e., P**2**(−)/(+) and P**2**o, decompose at a similar temperature, revealing that the thermolysis of the polymers is

**TABLE 5: Specific Optical Rotations of the Chiral Monomers and Their Helical Polymers in Different Solvents[a]**

| no. | polymer or monomer | $[\alpha]_D^{23}$, deg (*c*, g/dL) | | | |
|---|---|---|---|---|---|
| | | chloroform | dichloromethane | THF | toluene |
| 1 | P**1**(−) | +572.8 (0.050) | +578.8 (0.050) | +425.0 (0.05) | +571.4 (0.050) |
| 2 | **1**(−) | −15.5 (0.058) | | | |
| 3 | P**2**(−) | +529.8 (0.045) | +331.1 (0.045) | −153.9 (0.046) | −100.6 (0.052) |
| 4 | **2**(−) | −64.3 (0.056) | −52.0 (0.050) | −31.5 (0.054) | −64.0 (0.050) |
| 5 | P**2**(+) | +398.9 (0.061) | Δ | Δ | × |
| 6 | **2**(+) | +64.8 (0.054) | | | |
| 7 | P**2**o | −124.8 (0.050) | −132.2 (0.050) | +94.8 (0.050) | −135.6 (0.050) |
| 8 | **2**o | −22.8 (0.057) | −16.1 (0.056) | −5.5 (0.055) | −20.0 (0.055) |

[a] Debye solvent polarizability functions $[(\epsilon - 1)/(\epsilon + 2)]$:[19] chloroform, 0.71; dichloromethane, 0.73; THF, 0.68; toluene, 0.31. Abbreviations: Δ = partially insoluble, × = insoluble.

insensitive to the change in the pendant terminal groups but dependent on the type of amino acid attached to the polyene backbone.

Polymer P**1**(−) is completely soluble in common organic solvents including chloroform, toluene, THF, and dichloromethane. Polymers P**2**(−) and P**2**o show similar solubility. Intriguingly, however, P**2**(+) is completely soluble only in chloroform but totally insoluble in toluene, although its molecular structure is identical with that of P**2**(−) except for the chirality of the menthyl group. The reason for this solubility difference is unknown at present but may be associated with the differences in the chain stereoregularity and/or packing arrangements of the polymers in the solid state.

**Optical Rotation.** A polymer chain bearing chiral pendants can potentially exhibit very high optical activity, although racemization occurs in some polymer systems.[7−12] To check whether and how our polymers are optically active, we measured their specific optical rotations ($[\alpha]_D^{23}$) in different solvents. As can be seen from Table 5, all the polymers show large $|[\alpha]_D^{23}|$ values, indicating that they are highly optically active. The $[\alpha]_D^{23}$ values of the polymers are much higher than those of their corresponding monomers in the same solvents: e.g. the $[\alpha]_D^{23}$ value for the chloroform solution of P**1**(−) (+527.8°) is 30-fold higher than that for **1**(−) (−15.5°) in absolute terms. This suggests that the polymer chains take conformations with excesses of preferred handedness. Polymer P**1**(−) displays similarly high $[\alpha]_D^{23}$ values in chloroform, DCM, and toluene but a low $[\alpha]_D^{23}$ value in THF (Table 5, no. 1). It seems that there is little correlation between the Debye solvent polarity[19] and the specific optical rotation.

While monomers **2**(−) and **2**(+) show similar $[\alpha]_D^{23}$ values but opposite signs in chloroform, their polymers P**2**(−) and P**2**(+) show different $[\alpha]_D^{23}$ values but the same sign (Table 5, nos. 3−6). This implies that the optical activities of the polymers are determined by the helicity of their backbones (vide infra) and that the menthyl groups of different chiralities exert asymmetric forces of different directions on the chain helicities. Although the $[\alpha]_D^{23}$ values of **2**(−) and **2**o in chloroform possess the same sign, those of their polymers, viz. P**2**(−) and P**2**o, show opposite signs, suggesting that the bulkiness of the terminal group can affect the chain conformations, which in turn influences the optical rotations of the polymers.

Compared to P**1**, the optical rotations of P**2**, especially P**2**(−), are more susceptible to solvent change. The $[\alpha]_D^{23}$ value of P**2**(−) changes with solvent to a greater extent in both magnitude and sign than their monomers do. While chloroform and DCM are two solvents with similar properties, the $[\alpha]_D^{23}$ value of P**2**(−) in the former is 1.6-fold higher than that in the latter (Table 5, no. 3). Not only the magnitude but also the sign of the $[\alpha]_D^{23}$ value of the polymer is changed in THF and toluene. Since the $[\alpha]_D^{23}$ values of **2**(−) are negative in all solvents, the sign inversion observed in P**2**(−) in THF and toluene should be due to switching of the relative population of its left- and right-handed helical segments in these solvents. While the solvent effect on $[\alpha]_D^{23}$ of P**2**(+) cannot be examined because of its poor solubility, the $[\alpha]_D^{23}$ of P**2**o is found to vary with solvent. In the same solvent, the sign of $[\alpha]_D^{23}$ of P**2**o is generally opposite that of P**2**(−), indicating that the optical rotations of the amino acid-containing polyacetylenes can be altered by changing the bulkiness of their pendant terminal groups.

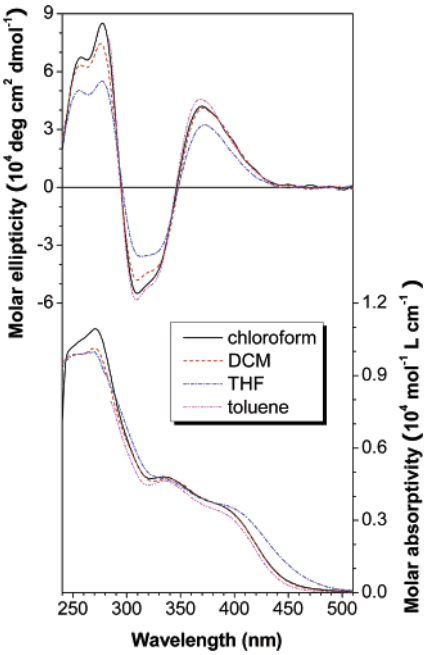


**Figure 5.** CD (upper panel) and UV spectra (lower panel) of P**1**(−) (sample from Table 1, no. 1) at 23 °C in different solvents. Polymer concentration (mM): 1.3 (CD) and 0.05 (UV). The spectral data in toluene below 283 nm were not taken due to the interference by the solvent absorption.

**Chain Helicity.** As discussed above, the high $[\alpha]_D^{23}$ values of the polymers imply that their chain segments take helical conformations. To confirm this, we conducted CD analysis, a powerful tool for studying helical structures.[20] The upper part of Figure 5 shows the CD spectra of P**1**(−) in different solvents. While monomer **1**(−) is CD inactive at wavelengths longer than 300 nm, strong Cotton effects are observed in the CD spectrum of P**1**(−) in chloroform at ∼310 and 368 nm, unambiguously proving that the polymer adopts a helical conformation with a preferred screw sense.

Proteins are natural polymers whose chain conformations vary with the changes in their surrounding environments such as medium (or "solvent"), pH, and temperature.[1,2] How will the

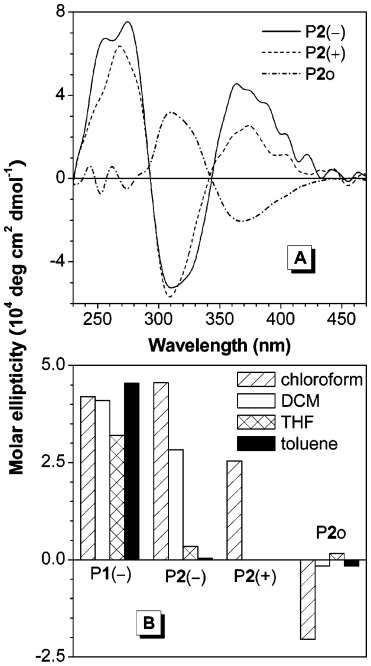


**Figure 6.** (A) CD spectra of P**2**(−) (sample from Table 2, no. 1), P**2**(+) (Table 3, no. 1), and P**2**o (Table 4, no. 1) in chloroform. (B) Variation of the first Cotton effects with solvents of P**1**(−) (data taken from Figure 5) at 370 nm, P**2**(−) at 364 nm, P**2**(+) at 374 nm, and P**2**o at 368 nm. Polymer concentration: ∼1.2−1.3 mM. Temperature: 23 °C.

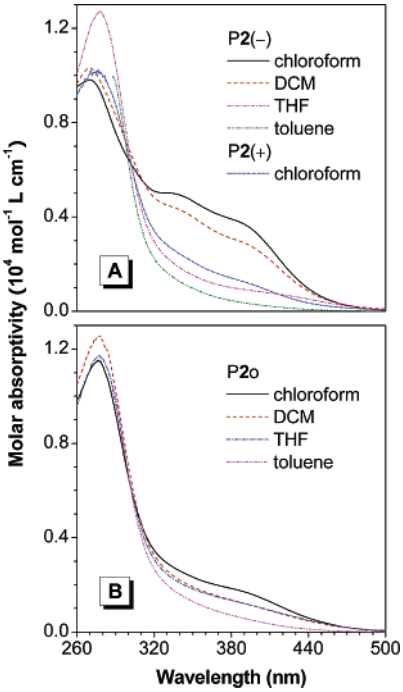


**Figure 7.** UV spectra of (A) P**2**(−) (sample from Table 2, no. 1) and P**2**(+) (Table 3, no. 1) and (B) P**2**o (Table 4, no. 1) in different solvents at 23 °C. Polymer concentration: ∼0.05 mM.

chain conformations of our polymers respond when the environmental conditions such as solvent are varied? Changing the solvent from chloroform to DCM and then to THF causes little change in the spectral profile of P**1**(−) (Figure 5). The peak intensity is, however, weakened, implying that a fraction of helical chain segments has reversed their screw senses. On the other hand, stronger Cotton effects are observed at similar wavelengths when the polymer is dissolved in toluene. Clearly, like proteins, P**1**(−) is also responsive to the variation in its environment.

The UV absorption spectra of P**1**(−) are shown in the lower panel of Figure 5. Its polyene backbone absorbs at ∼340 and 400 nm in chloroform. Similar spectra are obtained in DCM and toluene. The absorption spectrum of the polymer shifts to a slightly longer wavelength region in THF. Overall, the UV spectrum of the polymer is less susceptible to the solvent change than its CD spectrum. In other words, the CD analysis is a more sensitive tool for probing conformational change of a helical polymer.

Strong CD peaks associated with polyene backbone absorptions are also observed in other polymers (Figure 6). In chloroform, P**2**(−) exhibits a CD band with a high molar ellipticity ($[\theta] \sim 45\,000$ deg cm$^2$ dmol$^{-1}$) at ∼370 nm. The first Cotton effect of its cousin P**2**(+) locates at a slightly higher wavelength but with a lower molar ellipticity. The Cotton effects are further weakened with sign inversions when the pendant terminal groups are changed to octyl (P**2**o). Like P**1**(−), P**2**(−) and P**2**o also change their chain helicities with solvents. The ellipticity of the first Cotton effect of P**2**(−) decreases dramatically with no inversion in sign when the solvent is changed from chloroform to DCM, THF, and then toluene. A similar phenomenon is observed in P**2**o except that the sign is reversed in THF.

The UV spectra of P**2**(−) and P**2**o in different solvents are shown in Figure 7. In chloroform, the polyacetylene backbone of P**2**(−) absorbs strongly at 338 and 391 nm. In DCM, THF, and toluene, the spectrum blue-shifts with a progressive weakening in absorptivity. Unlike its congener P**2**(−), P**2**(+) absorbs little visible light in chloroform. For P**2**o, the strongest absorption is recorded in chloroform. The absorption spectrum measured in toluene is basically a structureless tail with low absorptivity.

**Acid-Induced Chromism.** It is well-known that conformations of proteins change with pH.[1] The changes in the NMR spectra of P**2**o induced by the addition of TFA (cf., Figures 2 and 3) suggest that the conformation of the polymer (hence its CD spectrum) will vary with the addition of the acid. This is indeed the case: addition of a small amount of TFA into the chloroform solution of P**1**(−) immediately weakens its CD signals (Figure 8A). Its molar ellipticity further decreases with increasing the amount of added TFA, with the first Cotton effect almost vanishing at ∼6 vol % of TFA.

The formation of regular helical structure is obviously entropically unfavorable. This entropic cost can, however, be partially compensated by the multiple intra- and interchain hydrogen bonds formed between the amino acid residues in the pendants of the polymer. The formation of the helical structure is thus a result of a subtle balance between these two antagonistic effects. As discussed in the Structural Characterization part, the TFA molecules may form hydrogen bonds with the amino acid appendages. This will break the balance, resulting in partial or full randomization of the polymer chains. The chain helicities of the leucine-containing polyacetylenes P**2** also become weaker upon TFA addition (Figure 8, panels B−D). In solutions with high acid concentrations, the Cotton effects at ∼370 nm completely disappear, while the broad CD peaks centered at ∼470 nm with the same or opposite signs emerge in the visible spectral region.

The dependence of the first Cotton effect of the polymers on the TFA concentration is summarized in Figure 9. When 2 vol % of TFA is added to the chloroform solution of P**1**(−), its ellipticity is decreased by 15%. When the TFA amount is

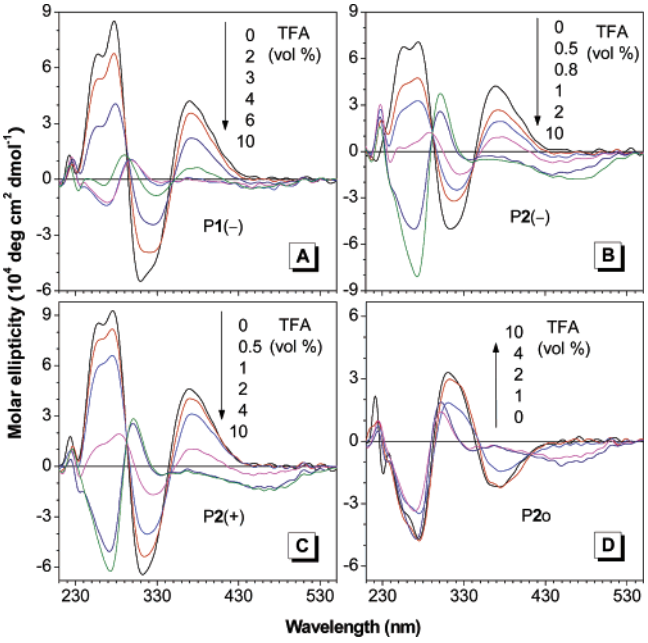


**Figure 8.** CD spectra of (A) P**1**(−) (sample from Table 1, no. 1), (B) P**2**(−) (Table 2, no. 1), (C) P**2**(+) (Table 3, no. 1), and (D) P**2**o (Table 4, no. 1) in trifluoroacetic acid (TFA)/chloroform mixtures with different volume fractions of TFA. Polymer concentration: ∼1.2−1.3 mM.

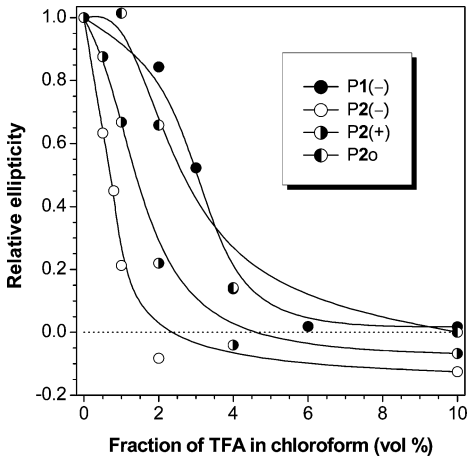


**Figure 9.** Effects of volume fractions of trifluoroacetic acid (TFA) on the relative molar ellipticities of P**1**(−) (sample from Table 1, no. 1) at 370 nm, P**2**(−) (Table 2, no. 1) at 369 nm, P**2**(+) (Table 3, no. 1) at 370 nm, and P**2**o (Table 4, no. 1) at 374 nm in TFA/chloroform mixtures. Polymer concentration: ∼1.2−1.3 mM.

doubled to 4%, the molar ellipticity is decreased not proportionally (by 30%) but exponentially (by 86%!). This is indicative of a cooperative process: once some chain segments are dissociated in chloroform through the breakages of the intrachain and interchain hydrogen bonds by the addition of an appropriate amount of TFA, the rest of the macromolecular chains are rapidly unfolded with the aid of entropy-driven chain randomization when a little more TFA is added.[3,10] Compared to that of P**1**, the helical conformations of polymers P**2** are more sensitive to perturbation by the acid. Cooperativity is again observed in these cases: the backbone CD absorptions of all the polymers drop dramatically in a narrow window of TFA concentration.

The addition of TFA into the polymer solutions also causes changes in their UV absorption spectra. The chloroform solution of P**1**(−) displays the polyene backbone absorptions at 340 and 400 nm (Figure 10A), which shift to longer wavelengths when

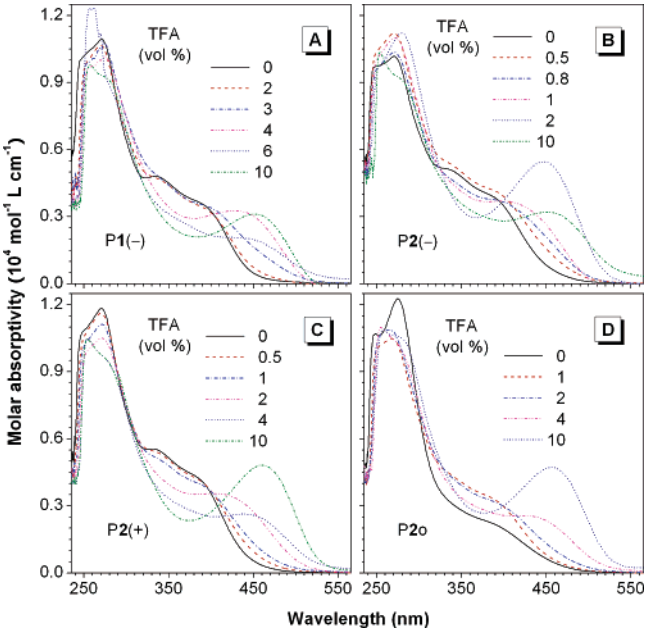


**Figure 10.** UV spectra of (A) P**1**(−) (sample from Table 1, no. 1), (B) P**2**(−) (Table 2, no. 1), (C) P**2**(+) (Table 3, no. 1), and (D) P**2**o (Table 4, no. 1) in trifluoroacetic acid (TFA)/chloroform mixtures with different volume fractions of TFA. Polymer concentration: ∼0.13−0.14 mM.

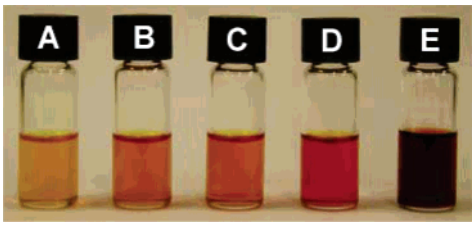


**Figure 11.** Photographs of chloroform solutions of P**2**(−) containing (A) 0, (B) 0.8, (C) 1, (D) 2, and (E) 10 vol % of trifluoroacetic acid. Polymer concentration: ∼50.3 mM.

TFA is added. Increasing the amount of the acid further red-shifts the spectrum, moving the absorption peak progressively to ∼480 nm. Similarly, the polyene backbone absorptions of other polymers red-shift with the addition of TFA. As discussed above, the disassembling of the polymer aggregates by the acid may enable the solvent molecules to better solvate the polymer chains. Such polymer chains may be better conjugated and exhibit higher absorptivity in the longer wavelength regions, hence the observed halochromism.

The changes in the absorption spectra of the polymers induced by the addition of TFA are so obvious that they can even be recognized by the naked eye (Figure 11). The color of a concentrated chloroform solution of P**2**(−) is yellowish orange. When a small amount of TFA is added, the color of the solution changes to orange. The solution color darkens progressively and turns to deep red when 10 vol % of TFA is added. The color change is reversible. Thus, in another set of experiments, a yellow solution of P**2**(−) turns orange red with the addition of the acid (Figure 12, panels A and B; note that the colors are lighter because the solutions are more dilute than those given in Figure 11). When the acid is gradually neutralized by adding an increasing amount of diethylamine (a base) into the solution, the color of the solution progressively returns to its original light color. The volatile acid can be driven out of the system by evaporation: the films obtained by casting solutions A and B have a similar light color (Figure 12, panels E and F), although

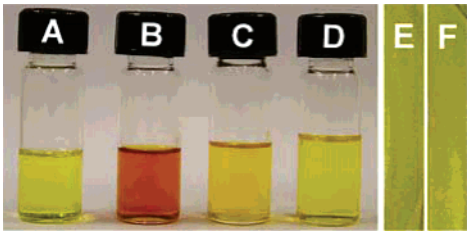


**Figure 12.** Photographs of the chloroform solutions of P**2**(−) (~12 mM) containing (A) 0 and (B) 10 vol % of TFA and TFA/diethylamine mixtures with (C) 2:1 and (D) 1:1 volume ratios and the thin solid films prepared by casting solutions of (E) A and (F) B on glass substrates.

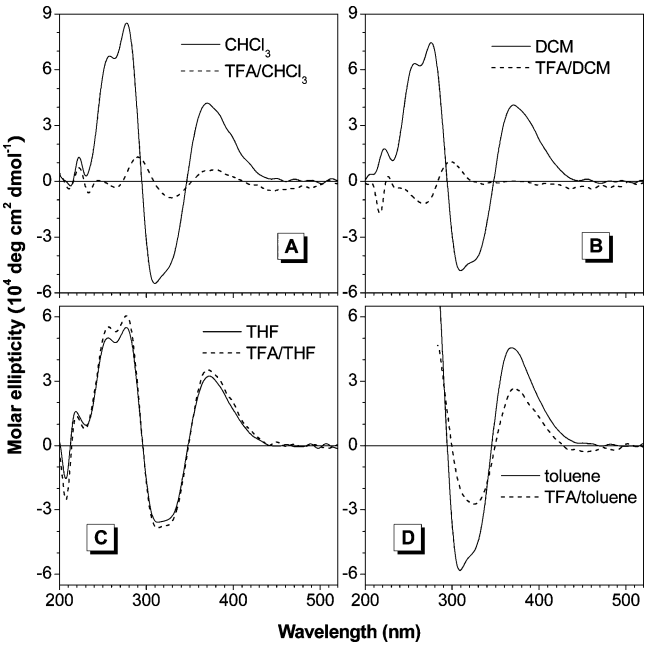


**Figure 13.** CD spectra of P**1**(−) (sample from Table 1, no. 1) in different solvents in the absence and presence of 4 vol % of trifluoroacetic acid (TFA). Polymer concentration: ~1.3 mM. The data below 290 nm in (D) were not taken due to the solvent interference.

the colors of their original solutions are very different. This proves that the acid-induced chromism is a readily reversible physical process, involving no irreversible degradative chemical reactions.

**Solvent Effect.** Is the halochromism only observable in chloroform? How will the solvent affect the chromic process? To answer these questions, we measured the CD spectra of P**1**(−) in different solvents containing 4 vol % of TFA. Similar to its solution in chloroform, the polymer exhibits weak CD signals in DCM in the presence of TFA (Figure 13). The effect of TFA on the CD spectrum of P**1**(−) in THF is, however, astonishingly different. The CD spectrum measured in the TFA/THF mixture is almost the same as that measured in pure THF. This high stability of the polymer helix against acid is truly impressive. The Cotton effects become weaker in toluene after the addition of TFA but the extents of the decreases are smaller, in comparison to those in the halogenated solvent systems. Clearly, the chromic process is greatly affected by the solvent.

Variations in the UV spectrum and solution color of P**1**(−) with solvent (Figure 14) agree well with those in its CD spectrum. The addition of TFA into the chloroform solution of the polymer red-shifts its backbone absorption to a longer wavelength ($\lambda_{max}$ = 450 nm), accompanied by a color change from orange to red (Figure 14A). At the same acid fraction, the

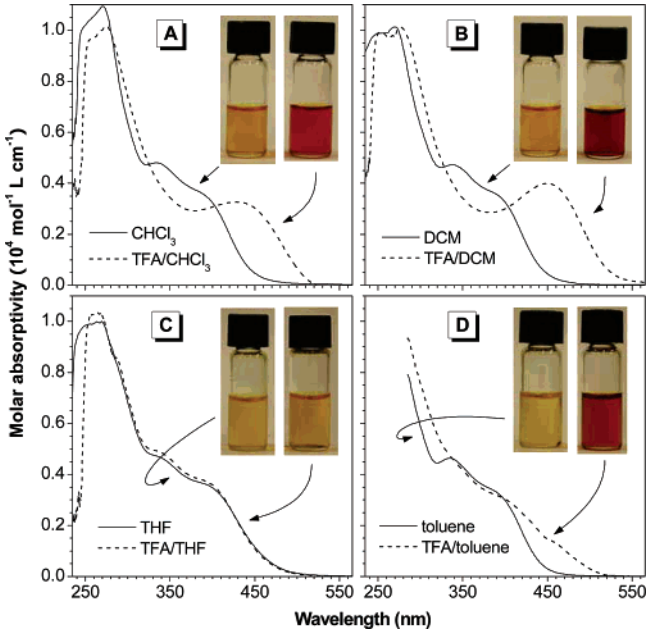


**Figure 14.** UV spectra and photographs of solutions of P**1**(−) (sample from Table 1, no. 1) without and with 4 vol % of TFA. Polymer concentration (mM): ~0.13 (spectra) and ~33.8 (photographs).

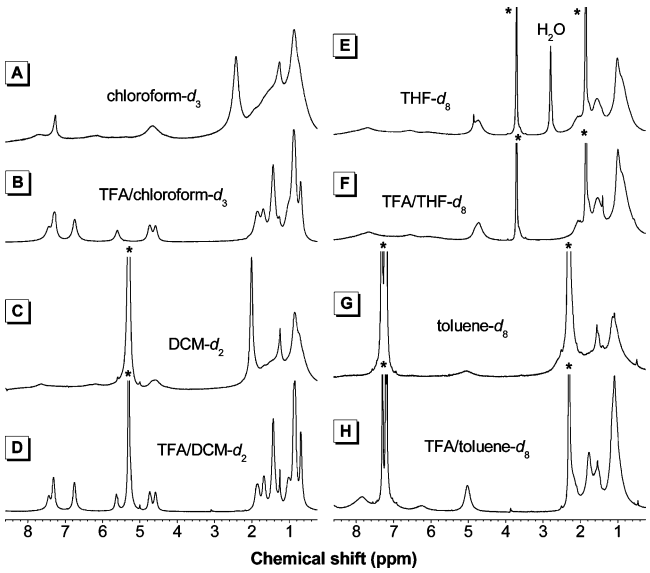


**Figure 15.** $^1$H NMR spectra of solutions of P**1**(−) (sample taken from Table 1, no. 1) in the absence and presence of 4 vol % of trifluoroacetic acid (TFA). Polymer concentration: 20 mg/mL. The solvent peaks are marked with asterisks.

polymer solution in the TFA/DCM mixture gives a stronger peak of the polyene backbone absorption at longer wavelength, as evidenced by the more intense color of the solution. In sharp contrast, the backbone absorption of the polymer and its solution color remain virtually unchanged with the addition of TFA into the THF solution. The polymer gives a red-shifted spectrum in the TFA/toluene mixture, in comparison to that recorded in pure toluene. The extent of the red-shift is, however, smaller than those observed in the halogenated solvents.

We studied the acid-induced conformational changes of P**1**(−) in the solvents by NMR spectroscopy. The polymer exhibits very broad proton resonance peaks in chloroform-*d*, due to the aggregation of the macromolecular strands aided by the hydrogen bond formation (Figure 15A).[3a,10,21] When the intra- and interstrand hydrogen bonds are broken by the addition of

the acid, sharper resonance peaks with fine structures emerge due to the better solvation of the polymer chains with more extended conformations in the TFA/chloroform mixture.[22]

The spectrum of P**1**(−) in DCM is even more poorly resolved (Figure 15C). There are almost no peaks in the downfield spectral region, where the polyene backbone and phenyl ring should resonate. This suggests that the polymer aggregates take a micelle-like structure, where the polyene backbone resides in the core. The physical forces experienced by the polymer in the constrained space of the core may force the polymer chains to bend, twist, and coil, thus limiting their effective conjugation lengths. On the other hand, the spectrum becomes better resolved with the addition of the acid, indicative of a greater extent of deaggregation. When the polymer is molecularly dissolved, its chains experience less constraint and can take more extended conformations with better $\pi$-conjugations. The combination of these two effects, i.e., the heavier aggregation (Figure 15C) and the greater deaggregation (Figure 15D), accounts for the observed larger changes in the CD and UV spectra of the polymer as well as in its solution color after TFA is added into the DCM solution.

Little change is observed, however, in the NMR spectrum of the polymer in the THF system: no peaks of the polyene backbone are recorded in the downfield spectral region even after the addition of TFA (Figure 15F). This is probably due to the stronger interaction between the polar solvent and the acid additive. The acid perturbs the chain conformation of P**1**(−) to a negligible extent in THF, hence the small changes observed in its CD and UV spectra and solution color in this solvent system.

Different from the THF system, addition of TFA into the toluene solution of P**1**(−) does enhance the resolution of its NMR spectrum (Figure 16H). However, almost no fine structures are observed in the spectrum in the TFA/toluene mixture, that is to say, the extent of resolution improvement is not as good as those observed in the halogenated solvent systems. This explains why the changes in the CD and UV spectra of P**1**(−) in the toluene system are between those of the above-discussed two extreme cases, viz., the remarkably large and negligibly small changes in the DCM and THF systems, respectively.

## Concluding Remarks

In this work, we synthesized a group of phenylacetylene derivatives bearing L-alanine and L-leucine moieties with different terminal groups and polymerized them into high molecular weight polymers in high yields. All the polymers take helical conformations, exhibiting large molar ellipticities associated with their backbone absorptions in the CD spectra. The chain helicities of the polymers are tunable by changing their molecular structures and environmental conditions.

The polymer containing the L-alanine moiety (P**1**) exhibits larger $[\alpha]^{23}_{D}$ and $[\theta]$ values than its congeners containing the L-leucine moiety (P**2**), manifesting the influence of the amino acid moieties on the helical conformations of the macromolecular chains. The smaller methyl group in the alanine moiety poses less steric hindrance, making it easier for the multiple hydrogen bonds to form in P**1**. The signs of the optical rotations and molar ellipticities of the polymer bearing the chiral, bulky (−)-menthyl group [P**2**(−)] are generally opposite those of its cousin bearing the achiral, slim octyl group (P**2**o), revealing that the chirality and bulkiness of the terminal group in the pendant play an important role in determining the helicity of the polymer chains.

The chain helicities of all the polymers change with the variations in their surrounding environments. Polymers P**2** are more susceptible to the external perturbations than P**1**: when the solvent is changed and the acid is added, the former shows larger changes in the $[\alpha]^{23}_{D}$ values and CD and UV spectra than the latter. One possible reason is that the hydrogen bonding in P**1** is tighter than that in P**2** because of the steric effect discussed above. Among P**2**s, the polymers carrying the chiral menthyl groups [P**2**(−)/(+)] are more sensitive to the perturbation caused by the acid addition than their counterpart carrying the achiral octyl group (P**2**o).

The polymers undergo continuous and reversible halochromic changes with the addition of TFA into, and removal of TFA from, their solutions. The halochromism is again susceptible to the variation in the solvent, due to the competition between the interactions of the acid with the solvent and the polymer, which affects the aggregations of the polymer chains and their backbone conformations in different solvents to varying extents. The novel halochromism of the polymers may find potential applications as colorimetric detectors in the chemical and ionic sensing systems.

**Acknowledgment.** This work was partly supported by the Research Grants Council of Hong Kong (HKU2/05C, 603505, 603304, and 664903), the 973 program of the Ministry of Science and Technology (2002CB613401), and the National Science Foundation of China (N_HKUST606_03). We thank Prof. Michael C. W. Chan of the Department of Biology and Chemistry of the City University of Hong Kong for his technical assistance in the elemental analysis of the monomers. B.Z.T. acknowledges the support of the Cao Guangbiao Foundation of Zhejiang University.

## References and Notes

(1) (a) Zubay, G. L. *Biochemistry*, 4th ed.; Wm. C. Brown Publishers: Boston, MA, 1998; Chapters 5 and 8. (b) Johnson, G. B. *The Living World*, 2nd ed.; McGraw-Hill: Boston, MA, 2000; Chapters 4 and 25.

(2) (a) Patzlaff, J. S.; Moeller, J. A.; Barry, B. A.; Brooker, R. J. *Biochemistry* **1998**, *37*, 15363. (b) Brizard, A.; Oda, R.; Huc, I. *Top. Curr. Chem.* **2005**, *256*, 167. (c) Fleishman, S. J.; Unger, V. M.; Ben-Tal, N. *Trends Biochem. Sci*. **2006**, *31*, 106.

(3) (a) Lam, J. W. Y.; Tang, B. Z. *Acc. Chem. Res*. **2005**, *38*, 745. (b) Rivera, J. M.; Craig, S. L.; Martin, T.; Rebek, J., Jr. *Angew. Chem., Int. Ed*. **2000**, *39*, 2130. (c) Nelson, J. C.; Saven, J. G.; Moore, J. S.; Wolynes, P. G. *Science* **1997**, *277*, 1793. (d) Green, M. M. *Angew. Chem., Int. Ed*. **1999**, *38*, 3139. (e) Yashima, E.; Maeda, K.; Okamoto, Y. *Nature* **1999**, *399*, 449.

(4) (a) Cha, J. N.; Stucky, G. D.; Morse, D. E.; Deming, T. J. *Nature* **2000**, *403*, 289. (b) Yu, S. M.; Soto, C. M.; Tirrell, D. A. *J. Am. Chem. Soc*. **2000**, *122*, 6552. (c) Chung, Y. I.; Christianson, L. A.; Stanger, H. E.; Powell, D. R.; Gellman, S. H. *J. Am. Chem. Soc.* **2000**, *120*, 10555. (d) Akagi, K.; Piao, G.; Kaneko, S.; Sakamaki, K.; Shirakawa, H.; Kyotani, M. *Science* **1998**, *282*, 1683.

(5) (a) Rowan, A. E.; Nolte, R. J. M. *Angew. Chem., Int. Ed*. **1988**, 37. (b) Zubarev, E. R.; Pralle, M. U.; Li, L. M.; Stupp, S. I. *Science* **1999**, *283*, 523. (c) Jenekhe, S. A.; Chen, X. I. *Science* **1999**, *283*, 372. (d) Whitesides, G. M.; Ismagilov, R. F. *Science* **1999**, *284*, 89. (e) Lashuel, H. A.; LaBrenz, R.; Woo, L.; Serpell, L. C.; Kelly, J. W. *J. Am. Chem. Soc*. **2000**, *122*, 5262. (f) Cheuk, K. K. L.; Li, B. S.; Tang, B. Z. *Curr. Trends Polym. Sci.* **2002**, *7*, 41.

(6) (a) McQuade, D. T.; Pullen, A. E.; Swager, T. M. *Chem. Rev.* **2001**, *101*, 2537. (b) Saxena, A.; Fujiki, M.; Rai, R.; Kim, S.-Y.; Kwak, G. *Macromol. Rapid Commun.* **2004**, *25*, 1771. (c) Jeong, K.-U.; Knapp, B. S.; Ge, J. J.; Jin, S.; Graham, M. J.; Harris, F. W.; Cheng, S. Z. D. *Chem. Mater.* **2006**, *18*, 680.

(7) (a) Ciardelli, F.; Lanzillo, S.; Pieroni, O. *Macromolecules* **1974**, *7*, 174. (b) Moore, J. S.; Gorman, C. B.; Grubbs, R. H. *J. Am. Chem. Soc*. **1991**, *113*, 1704. (c) Ciferri, A. *Macromol. Rapid Commun.* **2001**, *23*, 511.

(8) (a) Tang, B. Z.; Kotera, N. *Macromolecules* **1989**, *22*, 4388. (b) Tang, B. Z. *Polym. News* **2001**, *26*, 262. (c) Lam, J. W. Y.; Dong, Y.; Cheuk, K. K. L.; Tang, B. Z. *Macromolecules* **2003**, *36*, 7927. (d) Dong, Y.; Lam, J. W. Y.; Cheuk, K. K. L.; Tang, B. Z. *J. Polym. Mater*. **2003**, *20*, 189. (e) Lam, J. W. Y.; Dong, Y. P.; Cheuk, K. K. L.; Law, C. C. W.; Lai, L. M.; Tang, B. Z. *Macromolecules* **2004**, *37*, 6695.

(9) (a) Fukushima, T.; Takachi, K.; Tsuchihara, K. *Macromolecules* **2006**, *39*, 3103. (b) Zhao, H. C.; Sanda, F.; Masuda, T. *J. Polym. Sci. Part*

*A*: *Polym. Chem*. **2005**, *43*, 5168. (c) Sanda, F.; Terada, K.; Masuda, T. *Macromolecules* **2005**, *38*, 8149. (d) Onouchi, H.; Hasegawa, T.; Kashiwagi, D.; Lshiguro, H.; Maedak, K.; Yashima, E. *Macromolecules* **2005**, *38*, 8625. (e) Maeda, K.; Matsushita, Y.; Ezaka, M.; Yashima, E. *Macromolecules* **2005**, *38*, 4152. (f) Gal, Y. S.; Lim, K. T.; Shim, S. Y.; Kim, S. Y. H.; Koh, K.; Jang, S. H.; Jin, S. H. *Synth. Met*. **2005**, *154*, 169. (g) Akagi, K.; Guo, S.; Mori, T.; Goh, M.; Piao, G.; Kyotani, M. *J. Am. Chem. Soc*. **2005**, *127*, 14647. (h) Iwasaki, T.; Nishide. H. *Curr. Org. Chem*. **2005**, *9*, 1665. (i) Kang, S. W.; Jin, S. H.; Chien, L. C.; Sprunt, S. *Adv. Funct. Mater*. **2004**, *14*, 329. (j) Percec, V.; Obata, M.; Rudick, J. G.; De, B. B.; Glodde, M.; Bera, T. K.; Magonov, S. N.; Balagurusamy, V. S. K.; Heiney, P. A. *J. Polym. Sci. Part A*: *Polym. Chem*. **2002**, *40*, 3509.

(10) (a) Cheuk, K. K. L.; Lam, J. W. Y.; Chen, J.; Lai, L. M.; Tang, B. Z. *Macromolecules* **2003**, *36*, 5947. (b) Cheuk, K. K. L.; Lam, J. W. Y.; Lai, L. M.; Dong, Y.; Tang, B. Z. *Macromolecules* **2003**, *36*, 9752. (c) Li, B.; Cheuk, K. K. L.; Ling, L.; Chen, J.; Xiao, X.; Bai, C.; Tang, B. Z. *Macromolecules* **2003**, *36*, 77. (d) Li, B.; Cheuk, K. K. L.; Salhi, F.; Lam, J. W. Y.; Cha, J. A. K.; Xiao, K.; Bai, C.; Tang, B. Z. *Nano Lett*. **2001**, *36*, 323. (e) Li, B.; Kang, S.; Cheuk, K. K. L.; Wan, L.; Ling, L.; Bai, C.; Tang, B. Z. *Langmuir* **2004**, *20*, 7598. (f) Li, B.; Chen, J.; Zhu, C.; Leung, K. K. L.; Wan, L.; Bai, C.; Tang, B. Z. *Langmuir* **2004**, *20*, 2515.

(11) (a) Lai, L. M.; Lam, J. W. Y.; Cheuk, K. K. L.; Sung, H. H. Y.; Williams, I. D.; Tang, B. Z. *J. Polym. Sci. Polym. Chem*. **2005**, *43*, 3701. (b) Lai, L. M.; Lam, J. W. Y.; Tang, B. Z. *J. Polym. Sci., Part A*: *Polym. Chem.* **2006**, *44*, 2117.

(12) (a) Cheuk, K. K. L.; Tang, B. Z. In *Chromogenic Phenomena in Polymers*: *Tunable Optical Properties*; Jenekhe, S. A., Kiserow, D., Eds.; ACS Symp. Ser. No. 888; American Chemical Society: Washington, DC, 2005; Chapter 26, p 340. (b) Cheuk, K. K. L.; Li, B. S.; Tang, B. Z. In *Encyclopedia of Nanoscience and Nanotechnology*; Nalwa, H. S., Ed.; American Scientific Publishers: Stevenson Ranch, CA, 2004; Vol. 8, p 703. (c) Li, B.; Cheuk, K. K. L.; Chen, J.; Xiao, X.; Bai, C.; Tang, B. Z. In *Nano Science and Technology*−*Novel Structures and Phenomena*; Tang, Z. K., Sheng, P., Eds.; Taylor & Francis: London, UK, 2003; Chapter 9, p 98. (d) Tang, B. Z.; Cheuk, K. K. L.; Salhi, F.; Li, B.; Lam, J. W. Y.; Cha, J. A. K.; Xiao, X. In *Synthetic Macromolecules with Higher Structural Order*; Khan, I. M., Ed.; ACS Symp. Ser. No. 812; American Chemical Society: Washington, DC, 2001; Chapter 10, p 133.

(13) Tang, B. Z.; Poon, W. H.; Leung, S. M.; Peng, H. *Macromolecules* **1997**, *30*, 2209 and references therein.

(14) Tang, B. Z.; Kong, X.; Wan, X.; Feng, X.-D. *Macromolecules* **1997**, *30*, 5620 and references therein.

(15) Jones, J. *Amino Acid and Peptide Synthesis*; Oxford University Press: Oxford, UK, 1992; Chapter 19.

(16) (a) Umeda, Y.; Kaneko, T.; Teraguchi, M.; Aoki, T. *Chem. Lett.* **2005**, *34*, 854. (b) Mastrorilli, P.; Nobile, C. F.; Grisorio, R.; Rizzuti, A.; Suranna, G. P.; Acierno, D.; Amendola, E.; Iannelli, P. *Macromolecules* **2004**, *37*, 4488. (c) Schenning, A. P. H.; Fransen, M.; Meijer, E. W. *Macromol. Rapid Commun.* **2002**, *23*, 266. (d) Mitsuyama, M.; Konda, K. *Macromol. Chem. Phys.* **2000**, *201*, 1613. (e) Balcar, H.; Sedlacek, J.; Vohlidal, J.; Zednik, J.; Blechta, V. *Macromol. Chem. Phys.* **1999**, *200*, 2591. (f) Hirao, K.; Ishii, Y.; Terao, T.; Kishimoto, Y.; Miyatake, T.; Ikariya, T.; Noyori, R. *Macromolecules* **1998**, *31*, 3405. (g) Russo, M. V.; Iucci, G.; Furlani, A.; Camus, A.; Marsich, N. *Appl. Organomet. Chem.* **1992**, *6*, 517. (h) Yang, W.; Tabata, M.; Kobayashi, S.; Yokota, K.; Shimizu, A. *Polym. J.* **1991**, *23*, 1135.

(17) Percec, V.; Rudick, J. G.; Peterca, M.; Wagner, M.; Obata, M.; Mitchell, C. M.; Cho, W. D.; Balagurusamy, V. S. K.; Heiney, P. A. *J. Am. Chem. Soc.* **2005**, *127*, 15257.

(18) (a) Shirakawa, H. *Angew. Chem., Int. Ed*. **2001**, *40*, 2575. (b) MacDiarmid, A. G. *Angew. Chem., Int. Ed*. **2001**, *40*, 2581. (c) Heeger, A. J. *Angew. Chem., Int. Ed.* **2001**, *40*, 2591.

(19) (a) Chen, J. W.; Law, C. C. W.; Lam, J. W. Y.; Dong, Y.; Lo, S. M. F.; Williams, I. D.; Zhu, D.; Tang, B. Z. *Chem. Mater*. **2003**, *15*, 1535. (b) Lide, D. R. *CRC Handbook of Chemistry and Physics*; CRC Press: Boca Raton, FL, 1994; pp 6−155.

(20) (a) Nakanishi, K.; Berova, N.; Woody, R. W. *Circular Dichroism*: *Principles and Applications*; Wiley-VCH: New York, 2000. (b) Ciradelli, F.; Tsuchida, E.; Wohrle, D. *Macromolecular-Metal Complexes*; Springer: Berlin, Germany, 1996.

(21) Lam, J. W. Y.; Luo, J.; Dong, Y.; Cheuk, K. K. L.; Tang, B. Z. *Macromolecules* **2002**, *35*, 8288.

(22) Tonelli, A. E. *NMR Spectroscopy and Polymer Microstructure*: *the Conformational Connection*; VCH: New York, 1989.